

Structural Systematics. Part 5.¹ Conformation and Bonding in the Chiral Metal Complexes $[M(\eta^5-C_5R_5)(XO)Z(PPh_3)]^\dagger$

Stephanie E. Garner and A. Guy Orpen

School of Chemistry, University of Bristol, Bristol BS8 1TS, UK

Data were retrieved from the Cambridge Structural Database for 67 crystal structures containing suitable geometric data for 74 molecular fragments of the form $[M(\eta^5-C_5R_5)(XO)Z(PPh_3)]$ 1 ($X = C$ or N ; $Z =$ any ligand). These data were analysed to examine the conformational preferences for the triphenylphosphine ligand in respect of orientations about the $M-P$ bond and about the $P-C$ bonds of the attached phenyl groups, and the mechanisms by which the preferred conformers interconvert. There are two main diastereomeric conformers: group I which has S configuration at the metal and anticlockwise propeller (left-hand helix) conformation at PPh_3 ; and group II which has S configuration at the metal and clockwise propeller (right-hand helix) PPh_3 . Group I structures predominate in the available dataset (56 members to 18 in group II). In group I structures the phenyl group closest to the Z and XO ligands (ring B) of the PPh_3 ligand is on average rotated *ca.* 35° away from Z towards the XO ligand and is face-on to Z . In group II structures phenyl B is edge-on to Z and face-on to XO , on average being rotated a further 36° from Z . Analysis of the conformational data suggests the following order for the energy barrier of rotational processes involving the PPh_3 ligand: rotation about the $M-P$ bond $>$ PPh_3 helicity inversion by one-ring flip $>$ PPh_3 helicity inversion by asynchronous two-ring flip. Helicity inversion can occur *without* full rotation about the $M-P$ bond and is accompanied by a rocking about the $M-P$ bond. Full rotation about the $M-P$ bond takes place with concomitant PPh_3 helicity inversion. This analysis of experimental data provides a detailed test of a previous conformational model. The PPh_3 groups show distortions in $M-P$ and $P-C$ distances and $C-P-C$ angles consistent with significant and asymmetric $M-P$ π bonding in those complexes for which Z is a poor π acceptor and provide evidence for a model of PPh_3 π back bonding which involves participation of $P-C$ σ^* orbitals.

The use of transition-metal complexes in organic synthesis has attracted a great deal of interest in recent years.² The objective of much of this work has been the exploitation of an asymmetric metal centre as a chiral auxiliary to afford control of the stereochemistry of reactions taking place at organic ligands attached to the metal. Among a number of remarkable systems that have been developed two closely related classes of complexes of this type stand out: the iron carbonyl complexes $[Fe(\eta-C_5H_5)(CO)Z(PPh_3)]$ much studied in Oxford by Davies and his co-workers,³ and the rhenium nitrosyl species $[Re(\eta-C_5H_5)(NO)Z(PPh_3)]$ developed by Gladysz and his co-workers in Utah.⁴ Both these groups (and others exploring related chemistry)⁵ have established a substantial body of synthetic organic chemistry of the Z ligand perhaps most spectacularly in the case where the contact atom of Z is an sp^2 -hybridised carbon atom. Furthermore in a number of studies they have sought to establish the factors underpinning the stereoselectivity of the reaction chemistry of these and related species of the form $[M(\eta^5-C_5R_5)(XO)Z(PPh_3)]$ 1 ($X = C$ or N). For the most part these latter studies have focused on the conformational preferences of the Z ligand (see, *e.g.*, refs. 6–8) and in some cases explicitly assumed that the other ligands are innocent bystanders affording an essentially fixed asymmetric environment for the reactions at Z . In more recent work this approximation has been examined experimentally and theoretically and a more complete and detailed picture has begun to emerge.^{9,10}

In this paper we take the view (as have others^{1,11–13}) that one may learn about the favoured conformations of a (sub-)molecular fragment and the paths linking them by examining

those conformations actually observed for the fragment in the solid state in crystal structure analyses. We seek to identify the most common conformations of chiral complexes of type 1, focusing especially on the PPh_3 ligand, and the pathways linking these conformations, and to test the conventional wisdoms of the qualitative and quantitative conformational analyses that have been advanced for such systems. In carrying out this analysis we focus on the torsion angle data which describe these conformations. In addition we seek to test the proposition¹⁴ that metal-to-phosphine π donation causes distortions in the phosphine geometry and that such distortions should be asymmetric given the asymmetry of the metal–ligand unit in these complexes. Parts of this work have been reported in preliminary form.¹⁵ An earlier database study of PPh_3 conformations in $[M(\text{arene})LL'(PPh_3)]$ (arene = $\eta-C_5R_5$ or $\eta-C_6R_6$, L or $L' =$ any ligand) species is worthy of note.¹⁶

Experimental

Data Retrieval.—Crystal structures containing the molecular fragment $[M(\eta^5-C_5R_5)(XO)Z(PPh_3)]$ 1 ($X = C$ or N , $M =$ transition metal, $Z =$ any ligand) were located from the Cambridge Structural Database (CSD) using the QUEST program.¹⁷ Data for these crystal structures were retrieved from the January 1991 version of the CSD in which the master data file contained 86026 entries. The data files retrieved were screened manually and automatically and only structures which fulfilled all of the following criteria were retained for further analysis: (i) R factor ≤ 0.07 ; (ii) atomic coordinates included in the CSD; (iii) for multiple determinations of the same structure only the most accurate retained; and (iv) no disorder within the fragment. The final data files contained 74 fragments from 67 structures (see SUP 56917). A locally modified version of the program GEOSTAT¹⁸ was subsequently used to calculate the values of the torsion angles (τ_i , $i = 1-3$; ω_i , $i = 1-3$, see Fig. 1),

[†] Supplementary data available: (No. SUP 56917, 10 pp.): full references corresponding to CSD refiles. See Instructions for Authors, *J. Chem. Soc., Dalton Trans.*, 1993, Issue 1, pp. xxiii–xxviii.

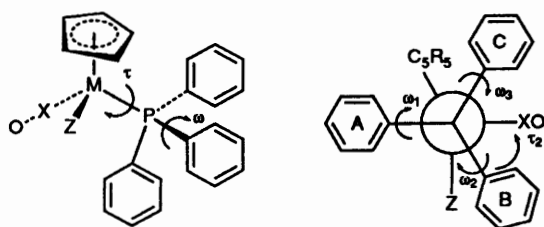


Fig. 1 Molecular fragment located from the CSD and definitions of phenyl ring nomenclature and torsion angles used

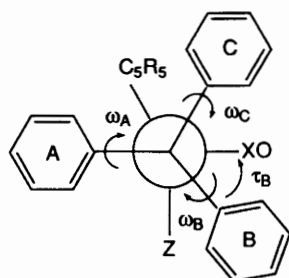
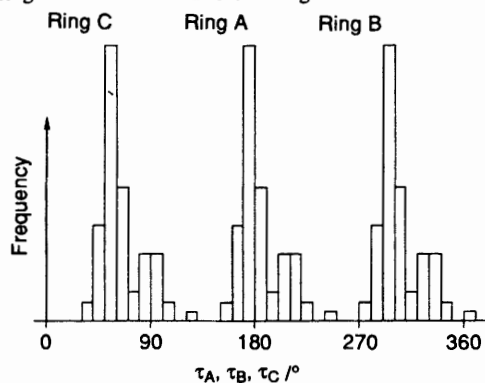


Fig. 2 Histogram of torsion angles τ_A , τ_B , τ_C and the fragment geometry corresponding to the popular conformation having $\tau_A \approx 180^\circ$

M–P and P–C bond lengths, C–P–C bond angles, and other parameters for each fragment.

The fragments were all referred to a common handedness at the metal (*S*, as illustrated in Fig. 1) and phenyl rings A–C labelled in the anticlockwise sense shown. The conformation of the phenyl groups of the PPh₃ ligand in respect of rotation about the M–P bond was described in terms of three torsion angles τ_i , $i = 1-3$ (X–M–P–C_{*ipso*}) for phenyl groups A–C respectively. The rings were defined such that ring A had τ_1 in the range 135–180 or -180 to -105° (i.e. a range equivalent to 135–255°), B had τ_2 in the range -105 to 15° and ring C had τ_3 in the range 15–135° a choice which is both convenient (see below) and ensures that ring B is that closest to the midpoint of the Z to XO region (which corresponds to $\tau = ca. -45^\circ$, see Fig. 2).

The conformational problem faced is essentially a four-dimensional one, in which we inspect the rotation of the PPh₃ ligand about the M–P bond and the rotation of each of the phenyl groups about their P–C_{*ipso*} bonds. Therefore we chose to represent this system in terms of four independent variables, τ , ω_A , ω_B , ω_C where $\tau = [(\tau_1 + \tau_2 + \tau_3)/3 + n360]$ (where, making use of the 360° periodicity of τ_{1-3} , n was set as required to put τ in the range 135–255°) and the ω_i values represent the orientations of the phenyl groups as described in the next paragraph. Defined in this way values of τ are inevitably very close to those of τ_1 but are averaged across the three phenyl groups. Such 'averaged' torsion angles τ_A , τ_B and τ_C where $\tau_A = \tau$, $\tau_B = \tau + 120^\circ$ and $\tau_C = \tau - 120^\circ$, are used for rings A–C respectively in all the discussion that follows. These torsion angle values all have periodicity of 360° of course.

The conformations of the phenyl groups in terms of the rotation about P–C_{*ipso*} bonds were defined in terms of torsion angles ω_A , ω_B and ω_C defined as $(\omega_{i1} + \omega_{i2} + 180)/2$ where ω_{i1} and ω_{i2} are the two M–P–C_{*ipso*}–C_{*ortho*} torsion angles of ring *i* calculated in the range -180 to 180° . Torsion angles ω_A , ω_B and ω_C therefore fall in the range 0–180° and have periodicity of 180°.

Results and Discussion

Of the 74 fragments studied, 35 have iron and 22 have rhenium as the transition metal, M. The other transition metals are: Ru (11 fragments), Os (1), Mn (2), W (1) and Cr (2). All but 14 of the fragments have an unsubstituted cyclopentadienyl ring. The exceptions are as follows: C₅H₄Me (4 fragments), C₅Me₅ (3), η^5 -menthylcyclopentadienyl (2), η^5 -indenyl (2), C₅H₄I (1), C₅H₄CHPh₂ (1) and C₅H₄Bu^t (1). The Z ligands are varied, and include acyl, alkyl, carbene, σ -vinyl and halide ligands (see Table 1). In 34 of the fragments the contact atom of Z is an sp²-hybridised carbon, e.g. as in an acyl or σ -vinyl ligand. The preponderance of these ligands mirrors the use of complexes of this sort for asymmetric synthesis.

The mean bond angles (and the standard deviations of the distributions*) at the metal for the 74 fragments are as follows: X–M–Z 93.9 (4.3), Z–M–Cp 119.6 (2.9), X–M–P 91.9 (2.1); X–M–Cp 125.6 (3.6), Z–M–P 91.8 (3.7) and P–M–Cp 124.7 (2.8)° (where Cp refers to the centroid of the η^5 -C₅ ring). These values are clearly in accord with Davies' repeated assertion^{3,6,10} that complexes of type 1 are best described as pseudo-octahedral with angles between the *fac* ligand set XO, Z and PPh₃ being close to 90° and the η^5 -C₅ ligand occupying the remaining three octahedral sites on the metal.

A histogram of the torsion angles τ_A , τ_B and τ_C (see Fig. 2) shows clear patterns of high and low frequency (which are essentially identical to those seen in a histogram of the 'unaveraged' torsion angles τ_1 , τ_2 and τ_3). In particular there are well defined regions of τ space in which no structures are found (3–36, 123–156 and 243–276°). Conversely the angle distribution shows maxima close to τ values of 60, 180 and 300° (the latter being equivalent to -60°). Such values correspond to an orientation of the PPh₃ ligand in which phenyl A is *anti* to the XO (carbonyl or nitrosyl) ligand and the B ring is close to the Z ligand. We therefore infer that such an orientation is energetically favoured and that the empty regions of τ space correspond to relatively high-energy conformations. The observation of large empty regions may further be taken as consistent with the existence of a significant barrier to rotation about the M–P bond in species of type 1, as has recently been observed in solution by NMR methods and postulated on the basis of molecular mechanics calculations for [Fe(η^5 -C₅H₅)(CO)(COMe)(PPh₃)] 2 and fluorinated analogues.¹⁰ Furthermore the vacant regions of τ space correspond to the highest-energy points on the calculated energy profile for rotation about the Fe–P bond in 2.

In fact the τ distribution is more complex than implied above, as is shown by closer inspection of the histogram, for example in the τ_B region (245–375°). Two peaks are visible corresponding to two groups of structures. The first and larger group (54 members) has τ_B values between 276 and 309° [mean 295(7)°] and a second smaller group (20 members) has τ_B values between 317 and 363° [mean 331(11)°], cf. the mean of the entire τ_B distribution 305(18)°. Note that corresponding values for the means and ranges of the τ_A and τ_C distributions can be generated from those for τ_B by subtracting 120 and 240° respectively.

To investigate the relationship between rotation of the PPh₃ ligand and individual phenyl group rotations, τ vs. ω scatter-

* Here and throughout this paper the number in parentheses following a mean value is the standard deviation of the distribution being described (and not the standard deviation of the mean itself).

Table 1 The CSD refcode,^a metal, XO, η^5 -C₅R₅, and Z ligands and group membership for the 74 fragments studied

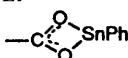
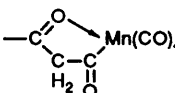
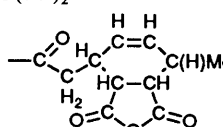
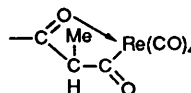
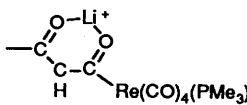
Refcode	M	XO	η^5 -C ₅ R ₅	Z	Group
BERMIU(1)	Mn	CO	C ₅ H ₄ Me	CO	I
BOBYAS	Re	NO	C ₅ H ₅	=C(H)Ph	I
BOBYEW	Re	NO	C ₅ H ₅	C(CH ₂ Ph)H(Ph)	I
BOFGOS	Fe	CO	C ₅ H ₅	SiPh(CH ₂) ₄ CH ₂	I
CAJFEY	Re	NO	C ₅ H ₅	N≡CC(Et)H(Ph)	I
CALWAN	Fe	CO	C ₅ H ₅	C(O)C(Me)H(Et)	I
CEMGAC	Ru	CO	C ₅ H ₄ (C ₁₀ H ₁₉) ^b	I	I
CICDUN	Fe	CO	C ₅ H ₅	C(OMe)=C(H)Me	I
CUXBIG	Fe	CO	C ₅ H ₅	C(O)CH ₂ C(OH)H(Ph)	I
CUYVIB	Re	NO	C ₅ H ₅	PPh ₂	I
DAWDUA	Fe	CO	C ₅ H ₅	C(O)EtC(OH)H(Me)	I
DEYCUF(1)	Ru	CO	C ₅ H ₇	PPh ₃	I
DEYKOH	Fe	CO	C ₅ H ₅	CF ₂	I
DICFAW	Re	NO	C ₅ H ₅	C(O)CH(Me)(CH ₂ Ph)	I
DOPHUL(1)	Ru	CO	C ₅ H ₅	PPh ₃	I
DOPHUL(2)	Ru	CO	C ₅ H ₅	PPh ₃	I
DUHXOT	Fe	CO	C ₅ H ₅	C(O)CH=CH(Me)	I
FAKYEV(1)	Cr	CO	C ₅ H ₅	CO	I
FALHAB	Re	NO	C ₅ H ₅	CH ₂ S(Me)CH ₂ Re(NO)(η -C ₅ H ₅)(PPh ₃)	I
FAMNAI	Fe	CO	C ₅ H ₅	C(O)CH ₂ C(NHPh)H(Ph)	I
FEBMAA	Fe	CO	C ₅ H ₅	C(=CH ₂)OZr(η -C ₅ H ₅) ₂ Cl	I
FEHTUH	Fe	CO	C ₅ H ₅	C(O)CH ₂ CHCH ₂ CH ₂	I
FELFOR	Fe	CO	C ₅ H ₅	C(O)CH ₂ =CHMe	I
FICSAL10	Fe	CO	C ₅ H ₅	CH ₂ SiMe ₃	I
FMCPRE10	Re	NO	C ₅ H ₅	C(O)H	I
FOBWUO10	Fe	CO	C ₅ H ₅	Et	I
FODLAL	Re	NO	C ₅ H ₅		I
FOYFUU	Re	NO	C ₅ Me ₅		I
FUDNUN10	Re	NO	C ₅ H ₅	ICH ₂ SiMe ₃	I
FUGWOT	Re	NO	C ₅ H ₅	CH=CHCH ₂ Ph	I
FUGWUZ	Re	NO	C ₅ H ₅	C(OMe)=CHCH ₂ Ph	I
FUVWAW	Re	NO	C ₅ H ₅	O=C(Me)Ph	I
GADWEN	Fe	CO	C ₅ H ₅	C(O)Me	I
GADWEN02	Fe	CO	C ₅ H ₅	C(O)Me	I
GAKJEH	Fe	CO	C ₅ H ₅	C(O)CHMeCH[OC(O)Ph](CH ₂) ₂ CH=CH ₂	I
GEFJEG	Re	NO	C ₅ H ₅	P(Bu) ^t ₂	I
GIBTUG	Fe	CO	C ₅ H ₅		I
GINTIG	Re	NO	C ₅ H ₅	=C=C(H)C ₁₀ H ₇ ^c	I
GINTOM	Re	NO	C ₅ H ₅	C≡CMe	I
JACXIU	Re	NO	C ₅ H ₅		I
JAGDAW	Fe	CO	C ₅ H ₅	N≡CMe	I
JAWKOH	Fe	CO	C ₅ H ₄ Me	C(O)Me	I
KARWOP	Re	NO	C ₅ H ₄ Me	I	I
KEHYEB	Fe	CO	C ₅ H ₅	N≡CCH[C(O)OH]CMe ₃	I
MCXCFE	Fe	CO	C ₅ H ₅	C(O)O(C ₁₀ H ₁₉)	I
MENCRU	Ru	CO	C ₅ H ₄ (C ₁₀ H ₁₉)	Cl	I
PFECYP(1)	Fe	CO	C ₅ H ₅	CO	I
SADTEW(1)	Re	NO	C ₅ H ₅	IRe(NO)(η -C ₅ H ₅)(PPh ₃)	I
SADTEW(2)	Re	NO	C ₅ H ₅	IRe(NO)(η -C ₅ H ₅)(PPh ₃)	I
SAYFIN	Fe	CO	C ₅ H ₅	C=CPhCPh=NO	I
SECHEN	Fe	CO	C ₅ H ₅	CH ₂ SCH ₂ Ph	I
SECHIR	Fe	CO	C ₅ H ₅	CH ₂ (O)Me	I
SELHEW	Ru	CO	C ₅ H ₅	C=CPhC(CF ₃) ₂ C(CN) ₂	I
VATDAV	Fe	CO	C ₅ H ₄ I	I	I

Table 1 (continued)

Refcode	M	XO	η^5 -C ₅ R ₅	Z	Group
VEDPAV	Re	NO	C ₅ Me ₅		I
ZEGJOK(1)	Fe	CO	C ₅ H ₅	CO	I
BERMIU(2)	Mn	CO	C ₅ H ₄ Me	CO	II
BIDYAO	Fe	CO	C ₅ H ₅	C(CO ₂ Et)=CMe ₂	II
BUVSOA	Re	NO	C ₅ H ₅	CH ₂ Ph	II
CAHYIT	Fe	CO	C ₅ H ₅	C(CO ₂ Et)=CHMe	II
CIBSFE	Fe	CO	C ₅ H ₅	SO ₂ (CH ₂ CHMe ₂)	II
CUNCOD	Ru	CO	C ₅ H ₅	C(OCHMe ₂)=CHPh	II
DEYCUF(2)	Ru	CO	C ₉ H ₇	PPh ₃	II
DUSYEV	Os	CO	C ₅ Me ₅	=C=C(Bu ^t)H	II
FAKYEV(2)	Cr	CO	C ₅ H ₅	CO	II
FUVPIV	Ru	CO	C ₅ H ₅	C(CO ₂ Me)=CH(CO ₂ Me)	II
JATYEI	Fe	CO	C ₅ H ₄ Bu ^t	I	II
PFECYP(2)	Fe	CO	C ₅ H ₅	CO	II
SELHIA	Ru	CO	C ₅ H ₅	C[C(CN) ₂]CPh=C(CF ₃) ₂	II
SELHOG	Ru	CO	C ₅ H ₅	C[C(CN) ₂]CMe=C(CF ₃) ₂	II
TPCPTW	W	CO	C ₅ H ₅	≡CSPH	II
VADCEI	Fe	CO	C ₅ H ₅	CMe=CMe(C ₂ B ₄ H ₅ Et ₂)	II
VATDEZ	Fe	CO	C ₅ H ₄ C(H)Ph ₂	I	II
ZEGJOK(2)	Fe	CO	C ₅ H ₅	CO	II

^a Multiple fragments from one refcode are indicated by numbers in parentheses. ^b C₁₀H₁₉ = menthyl. ^c C₁₀H₇ = naphthyl.

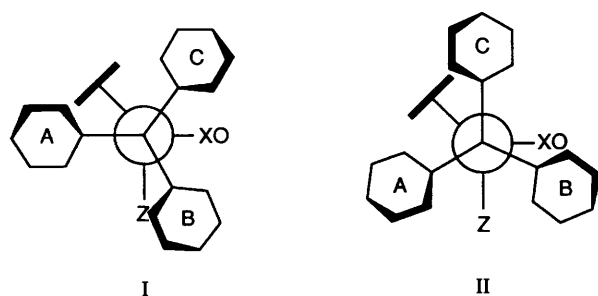
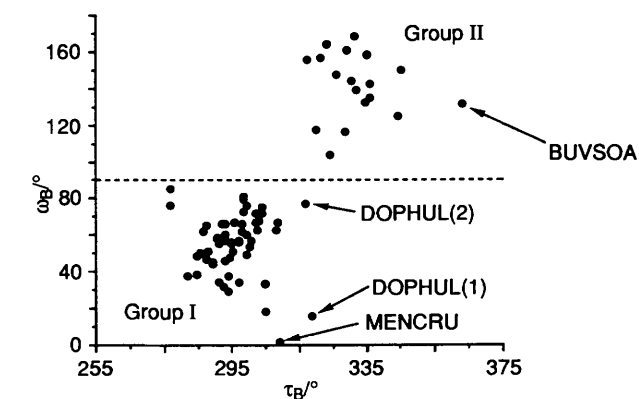


Fig. 3 Scattergram of torsion angle ω_B vs. τ_B for all structures indicating the two main structure types, groups I and II; schematic representations of the two conformer types. The CSD refcodes of structures which lie between the main concentrations of points are indicated

plots were drawn (Figs. 3 and 4). In Fig. 3 the relationship between τ_B and ω_B is illustrated. Clearly there are sizeable regions in which no structures are observed. Furthermore the structures fall into two groups on the basis of their ω_B values. The larger (56 members) group has ω_B values in the range 2–86° while the smaller (18 members) has ω_B values in the range 103–168°. These groups, which are termed I and II in the discussion below, are almost exactly coincident (barring two fragments, both from CSD refcode DOPHUL, which have τ_B

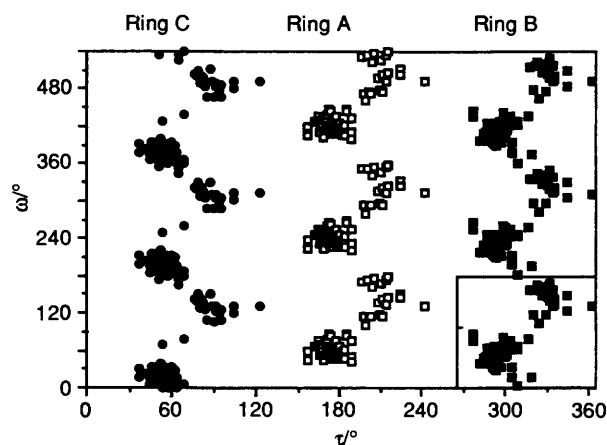


Fig. 4 Scattergram of torsion angles ω_i vs. τ_i ($i = A, B$ or C) for the three phenyl groups of the PPh₃ ligands. Three regions (0–180, 180–360, 360–540°) equivalent to one another due to the 180° periodicity of ω are included. The unique region of ω_B vs. τ_B space as shown in Fig. 3 is boxed

ca. 318°, see below) with those noted above on the basis of the τ_B values. The 'average' conformations for the two groups may be represented by the mean τ and ω values of the two sets of conformations: group I, τ_A 176(8), τ_B 296, τ_C 56, ω_A 63(19), ω_B 55(17), ω_C 33(43)°; group II, τ_A 212(11), τ_B 332, τ_C 92, ω_A 144(24), ω_B 141(18), ω_C 127(12)°. The conformations corresponding to these values are illustrated schematically in Fig. 3.

Several points emerge from these observations. First the two groups of structures have different arrangements of the phenyl ring (B) close to the Z ligand. Group I structures conform to the simplified early conformational model of Davies *et al.* [*e.g.* ref. 6(a)] for species such as I in that they have phenyl group B face-on to the Z ligand and more nearly eclipsing Z. In the simplest such model, with phenyl B exactly eclipsing Z and perfectly face-on, we would have τ_B *ca.* 270° and ω_B *ca.* 90°. This is a conformation that does not occur in our set of data. At the centroid of group I (τ_B 296° and ω_B 55°) rotations about the M–P and P–C bonds have combined to produce a conformation (see Fig. 2) that still shields one face of the Z ligand. In contrast conformations in group II structures are

qualitatively different, having the B ring closer to eclipsing the XO ligand and essentially face-on to XO but more nearly edge-on to the Z ligand (ring A is now more nearly face-on to Z). The correlation between the conformations of different phenyls is strong as we show below and the ω values in two groups correspond to conformations close to the two enantiomeric C_3 helical propeller conformers of the PPh_3 group which have ideal ω_i values of 40, 40, 40° and 140, 140, 140° respectively,¹² cf. the group centroid values of 63, 55, 33° for I and 144, 141, 127° for group II. Thus groups I and II correspond to the two diastereomeric species in which the *S* configuration at the metal is coupled with anticlockwise screw (*i.e.* left-handed helix) (I) or clockwise screw (*i.e.* right-handed helix) (II) propeller conformations of the PPh_3 group. Davies *et al.*¹⁰ have estimated the energy difference between group I and II conformers of $[Fe(\eta-C_5H_5)(CO)(COMe)(PPh_3)]$ to be ca. 1 kcal mol⁻¹ (*ca.* 4.184 kJ mol⁻¹) a value which suggests a ratio of the two diastereomers of *ca.* 5:1 at room temperature, fortuitously¹⁹ close to that observed for group I and II structures here (56:18, *ca.* 3.1:1).

One key question (that may have a bearing on the stereoselectivity of the reactions of these species) is why do some occur as group I and others as group II diastereomers? Further one might ask is the result an inherent consequence of the molecular connectivity or can the crystal environment cause one form to occur in the solid while the other predominates in solution? We note that while one cannot draw inferences on the relative energies of the two types of structure (I and II) from the numbers of examples seen, it can safely be assumed that the two diastereomers will normally have rather similar energies. In addition in cases studied to date (see ref. 10 for a critical review of the NMR and other data on this point) they are apparently in rapid equilibrium in solution on the NMR time-scale at all temperatures studied. Inspection of Table 1 yields only limited conclusions as to the answers to these questions. Thus of the 60 cases where C_5R_5 in 1 is C_5H_5 , 47 are in group I and 13 in II (ratio 3.7:1), of the 35 cases where $M(XO) = Fe(CO)$ 28 are in group I and 8 in II (ratio 3.5:1), of the 22 cases where $M(XO) = Re(NO)$, 21 are in group I and only 1 (CSD refcode BUVSOA which has a highly atypical τ_B value, 362.9°, see Fig. 3) in II (ratio 21:1) and of the 15 cases where $Z = C(O)R$, *i.e.* acyl, all 15 have group I conformations. While we hesitate to draw *any* conclusions about energetics from the numbers of structures¹⁹ it seems that rhenium nitrosyl species and acyl complexes may prefer group I conformations more strongly than other sub-classes of complexes of type 1. Why this should be so cannot be deduced from this evidence.

The cases in which a single compound gives rise to two or more fragments listed in Table 1 include two 'non-chiral' species, in which $Z = PPh_3$ (CSD refcodes DEYCUF and DOPHUL). Of these cases one $\{[Ru(\eta^5-C_9H_7)(CO)(PPh_3)_2]ClO_4 \cdot CH_2Cl_2$, CSD refcode DEYCUF} gives rise to one fragment in group I and a second in II. The other cases also include those in which there are either two crystallographically independent $[M(\eta^5-C_5R_5)(XO)Z(PPh_3)]$ units per unit cell (CSD refcode SADTEW, for which the fragments are part of a dimeric molecule) or more than one crystal form known (CSD refcodes GADWEN and GADWEN02). Finally, four compounds (CSD refcodes BERMIU, FAKYEV, PFECYP and ZEGJOK) contribute one fragment to each of groups I and II simply because they have $Z = XO = CO$ and perforce have both 'diastereomers' present. Therefore in no case in Table 1 have pure 'crystal packing effects' clearly been observed to be sufficient to overcome conformational preferences inherent in the molecular connectivity (although the situation is not clear for CSD refcode DEYCUF).

Fig. 4 shows a scatterplot of τ vs. ω for all three rings A–C allowing for the 180° periodicity of the ω values and therefore including three equivalent regions of ω space, *i.e.* 0–180, 180–360 and 360–540°. Particularly notable is the near-continuous nature of the ω distributions for the three different rings and the

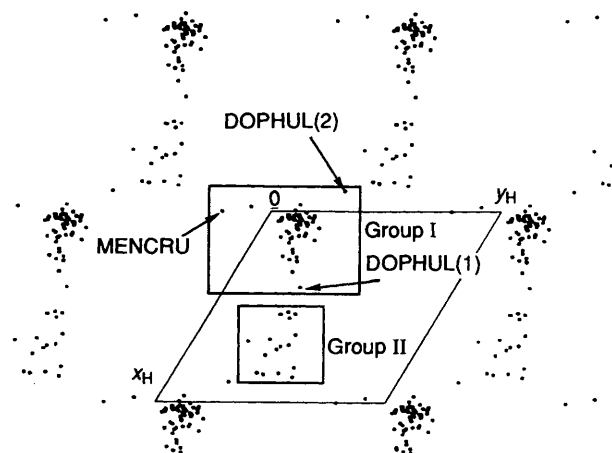


Fig. 5 Scattergram of torsion angles ($\omega_A, \omega_B, \omega_C$). A slab of the three-dimensional conformation space (x_H, y_H, z_H) and its unit cell viewed down the z_H axis that trisects $\omega_A, \omega_B, \omega_C$ are shown. All fragments that have z_H values between 0 and 0.333 are shown (in fact all lie in the range $0.055 < z_H < 0.30$). The two unique groups of conformations I and II are shown and the CSD refcodes of three structures which lie between the main concentrations of points are indicated

correlation of ω and τ values which leads to the zigzag patterns of points up the ω axis of the plot. The inference to be drawn is that rotation of the phenyl groups about their $P-C_{ipso}$ bonds is subject to a relatively small energy barrier (*cf.* the larger empty regions in τ space and higher barrier inferred). This conclusion is entirely consistent with the recent NMR studies of Davies *et al.*¹⁰ The zigzag pattern suggests that the PPh_3 group must oscillate about the $M-P$ bond during the rotation of the phenyl groups. Davies *et al.*¹⁰ arrived at a similar conclusion (magnitude of oscillation $\pm 45^\circ$), based on molecular modelling calculations on complex 2.

In order to assess the correlations between the ω values themselves the distribution of points was represented as a scatterplot on three axes (x_H, y_H, z_H) originally devised by Dunitz and co-workers¹² in their study of the conformation of the phenyl rings of PPh_3 species (especially $OPPh_3$) in crystal structures. They exploited the periodicity and symmetry of the torsion angle space ($\omega_A, \omega_B, \omega_C$) which is described by the crystallographic space group $R32$. They further showed that if the torsion angle distribution was shown using axes corresponding to the hexagonal setting of this space group (x_H, y_H, z_H), then the points all fell in well separated layers with approximately constant values of z_H (*ca.* $\frac{1}{6}, \frac{1}{2}, \frac{5}{6}$, etc.). While the ($\omega_A, \omega_B, \omega_C$) space in our system does not have three-fold (or indeed any rotational) symmetry, the torsion angle data can be represented in the same way on hexagonal axes (corresponding to the non-standard crystallographic space group $R1$!) with unit-cell dimensions $a = b = 180 \cdot \sqrt{2} = 254.6$, $c = 180 \cdot \sqrt{3} = 311.77^\circ$, $\alpha = \beta = 90^\circ, \gamma = 120^\circ$ and fractional coordinates derived using the following relationships: $x_H = (2\omega_A - \omega_B - \omega_C)/540$, $y_H = (\omega_A + \omega_B - 2\omega_C)/540$ and $z_H = (\omega_A + \omega_B + \omega_C)/540$.²⁰ In this representation there are three equivalent conformations per $R1$ unit cell with coordinates (x_H, y_H, z_H), $(\frac{2}{3} + x_H, \frac{1}{3} + y_H, \frac{1}{3} + z_H)$ and $(\frac{1}{3} + x_H, \frac{2}{3} + y_H, \frac{2}{3} + z_H)$. Fig. 5 shows the distribution of points for a slab of this hexagonal space with $0 \leq z_H \leq \frac{1}{3}$, as viewed down the z_H axis. As for the study¹² on $OPPh_3$ there are layers near $z_H = 0, \frac{1}{3}$ and $\frac{2}{3}$ which are clear of any points (see Fig. 6 for a view parallel to these layers). The two groups of structures I and II noted in Fig. 3 are identified on Fig. 5. It is also clear that there are large regions clear of points within the slab shown in Fig. 5 which are centred at approximately $x_H = \frac{1}{3}, y_H = \frac{2}{3}, z_H = \frac{1}{6}$. These forbidden regions correspond to conformations in which ($\omega_A, \omega_B, \omega_C$) are close to (90, 90, -90°) (see below). The populated regions are similar but not identical to those observed by Dunitz and co-workers¹² in their study of $OPPh_3$ species. Thus the coordinates (x_H, y_H, z_H) of the

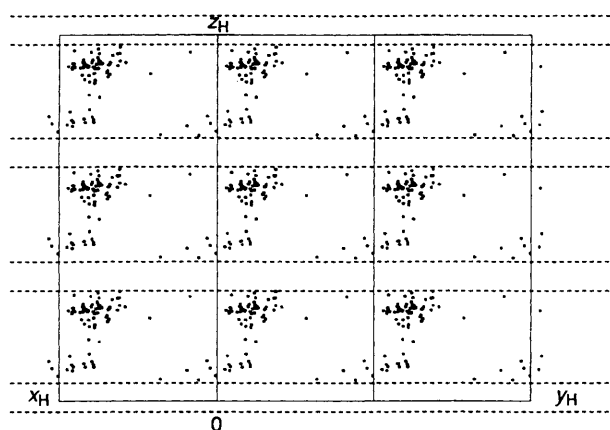


Fig. 6 Scattergram of torsion angles (ω_A , ω_B , ω_C). A slab of the three-dimensional conformation space (x_H , y_H , z_H) and its unit cell viewed perpendicular to the y_H and z_H axes are shown. The empty regions close to $z_H = 0, \frac{1}{3}, \frac{2}{3}$ and 1 are indicated

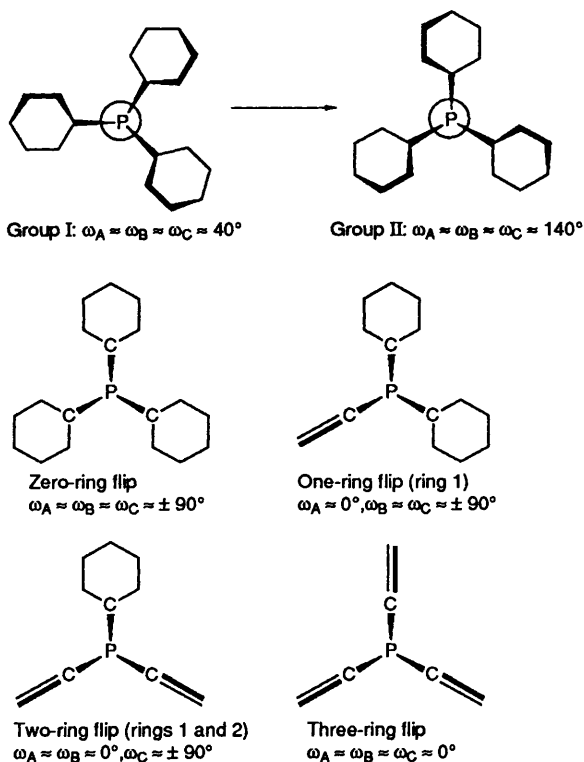


Fig. 7 The stereoisomerisation reaction interconverting the helical propellers of group I and II structures and the idealised ring-flip mechanisms through which it might occur

centroids of groups I and II in the present work are (0.07, 0.096, 0.28) and (0.71, 0.39, 0.10) respectively, compared with those for OPPh_3 , (0, 0, 0.22) and (0.66, 0.33, 0.11). Note in particular that there is enhanced variation in the z_H coordinate as well as deviations from the ideal C_3 symmetric conformations in the system studied here.

We now turn to the details of the mechanism(s) by which structures of type I stereoisomerise into type II and the related questions of the mechanism of helicity inversion of the PPh_3 conformation and consequences of full rotation about the M–P bond in these species. The description of conformational behaviour in aryl-substituted species is usually framed in the terminology of Kurland and co-workers,²¹ in which idealised reaction paths are classified according to the number of aryl groups which ‘flip’ during the process. In terms of the parameters used in this study this means the number of phenyl groups whose ω_i passes through 0° (or $\pm 180^\circ, \pm 360^\circ$, etc.) while

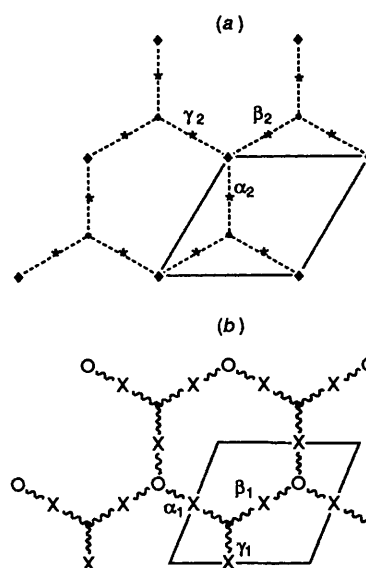


Fig. 8 Paths for interconversion of PPh_3 conformers: (a) a view of the (x_H , y_H , z_H) unit cell down z_H showing the positions of idealised propeller and two-ring flip conformers close to $z_H = \frac{1}{6}$; (b) a view of the (x_H , y_H , z_H) unit cell and the positions of idealised propeller and one-ring flip conformers close to $z_H = 0$. \blacklozenge , $\omega_{A-C} = 40 \pm (0, 180, \text{etc.})^\circ$, $z_H = 0.22$; \bullet , $\omega_{A-C} = -40 \pm (0, 180, \text{etc.})^\circ$, $z_H = 0.11$; $*$, two-ring flip intermediate, $z_H = 0.167$; \times , one-ring flip intermediate, $z_H = 0.0$; \circ , $\omega_{A-C} = 40 \pm (0, 180, \text{etc.})^\circ$, $z_H = 0.11$; $---$, two-ring flip pathway at $z_H = 0.167$; $\sim\sim\sim$, one-ring flip pathway through $z_H = 0.0$

the other two ω_i values pass through $\pm 90^\circ$ during the change from group I to II conformations. The full range of possible idealised intermediate geometries from zero through one-, two- and three-ring flip is illustrated in Fig. 7. The zero-ring flip positions in ω space correspond to the centres of the large discoid empty regions noted above (e.g. near $x_H = \frac{1}{3}$, $y_H = \frac{2}{3}$, $z_H = \frac{1}{6}$) and may therefore be discounted as possible intermediates. The three-ring flip position ($\omega_A \approx \omega_B \approx \omega_C \approx 0^\circ$) corresponds to another empty region of ω space close to the origin of the (x_H , y_H , z_H) unit cell and can therefore also be discounted. Fig. 8 shows the positions in the (x_H , y_H , z_H) unit cell corresponding to one- and two-ring flip intermediate geometries. Note that there are three distinct two-ring flip paths [α_2 , β_2 and γ_2 in Fig. 8(a)], geometries on the paths from group I to II structures in which different combinations of rings are flipped (for path α_2 , rings B and C flip; for β_2 , rings A and C; and for γ_2 , rings A and B). Similarly there are three distinct one-ring flip paths [for α_1 , ring A flips; for β_1 , B; and for γ_1 , C, see Fig. 8(b)].

The idealised one-ring flip geometries lie in the empty regions of (x_H , y_H , z_H) space around $z_H \approx 0, \frac{1}{3}, \frac{2}{3}$. In contrast the two-ring flip geometries lie in the heavily populated layers close to $z_H \approx \frac{1}{6}, \frac{1}{2}, \frac{5}{6}$. On this basis and the near-continuous nature of the distribution of points within these layers (see Fig. 5) the two-ring mechanism seems likely to be the lowest-energy process by which the chirality of the PPh_3 propeller in complex 1 can be inverted. However as shown in Fig. 6 and noted above the description of the ω space by a two-dimensional projection is an approximation which ignores the substantial fluctuations up and down z_H . The consequence of these fluctuations is that the empty layer at $z_H \approx 0, \frac{1}{3}, \frac{2}{3}$ is rather thin (e.g. not as thick as in the case of OPPh_3 species) and pathways which cross this layer cannot be ruled out. Fig. 9 shows one region of the (x_H , y_H , z_H) unit cell where the populated regions (above and below $z_H = 0$) are particularly close to one another either side of one-ring flip positions in which either ring A or B (but not C) is flipped. We therefore infer from these observations that one-ring flip mechanisms may be operative in species 1 but they are likely to be higher in energy than the two-ring flip processes.

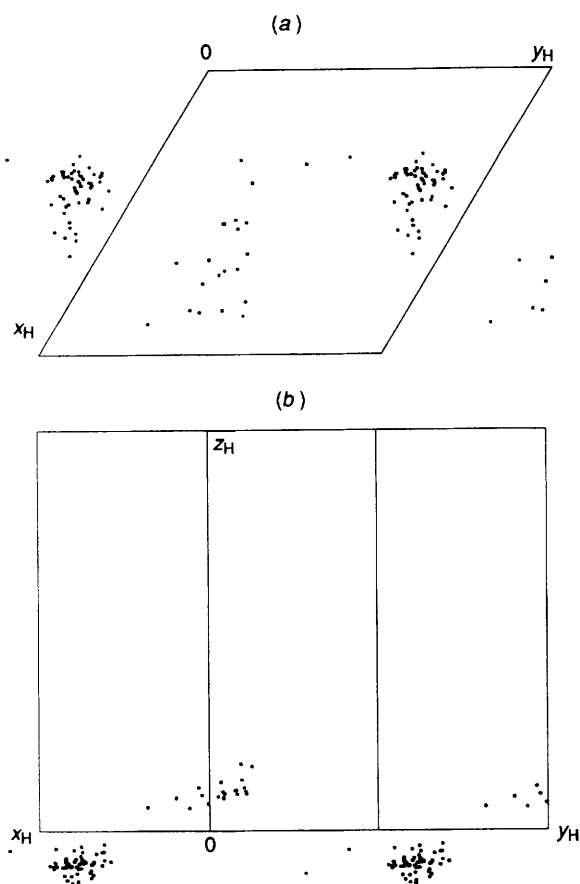


Fig. 9 Scattergrams of torsion angles (ω_A , ω_B , ω_C). A slab of the three-dimensional conformation space (x_H , y_H , z_H) and its unit cell viewed (a) down the z_H axis (cf. Fig. 5), (b) perpendicular to the y_H and z_H axes (cf. Fig. 6). Only fragments that have z_H values between -0.167 and 0.167 are shown

The mechanism of interconversion of clockwise and anti-clockwise PPh₃ propeller conformations in OPPh₃ species was the subject of a structure correlation study by Dunitz and co-workers¹² who concluded that in that, more symmetrical, case there was clear evidence from the structural data to support a two-ring flip mechanism. Davies *et al.*¹⁰ have studied the mechanisms of M-P and P-C rotation for [Fe(η -C₅H₅)(CO)(COMe)(PPh₃)] by means of molecular mechanics calculations and suggested for species such as **1** that a sequence of one- and two-ring flips were involved in full (*i.e.* 180° rotation of the phenyl rings). This is not necessarily the case since a series of two-ring flips will also give rise to 180° rotation of all three phenyl groups. Furthermore the calculations of Davies *et al.*¹⁰ suggested that the two-ring flip should encounter a lower energy barrier (*ca.* 3 kcal mol⁻¹) than the one-ring flip (*ca.* 5 kcal mol⁻¹) a prediction which is entirely in accord with our observations above.

The correlation of rotation about the M-P bond with the process of PPh₃ helicity inversion is apparent from the identification of groups I and II. As noted above there is near-perfect matching between the groups of structures selected on the basis of their τ_B values and those selected on the basis of their ω_B values. The only exceptions arise from bis(triphenylphosphine) species {[Ru(η -C₅H₅)(CO)(PPh₃)₂]BPh₄, CSD refcode DOPHUL} which yields two fragment geometries which are atypical in having τ values typical of the low end of the group II range but ω_B values close to those of the remainder of group I. In fact these two geometries are more truly intermediate between the two main groups in ω space (see Fig. 5). As such they (and the other indicated fragment in Fig. 5, CSD refcode MENCURU) are models for the midpoints of

the helicity inversion of the PPh₃ ligand by the three different two-ring flips possible in **1** [α_2 , β_2 , γ_2 in Fig. 8(a)]. The τ_B values for these three fragments are not dissimilar [DOPHUL(1) 318.6, DOPHUL(2) 317.0, MENCURU 309.0]°. Apparently this (*i.e.* τ_B *ca.* 315°) is an orientation which allows helicity inversion of PPh₃ to take place by any of the three different routes. The ω values for these three fragments seem to indicate that the two-ring flip process is not synchronous in this system. Thus for MENCURU the ω values are 41, 2, 79° (*cf.* 'ideal' values for the corresponding two-ring flip species γ_2 which lies between 40, 40, 40 and $-40, -40, 140^\circ$, *i.e.* of 0, 0, 90°). For DOPHUL(1) the ω values are 101, 16, -30° (*cf.* 'ideal' values for the corresponding two-ring flip species α_2 which lies between 40, 40, 40 and 140, $-40, -40^\circ$, *i.e.* of 90, 0, 0°). For DOPHUL(2) the ω values are $-9, 77, -37^\circ$ (*cf.* 'ideal' values for the corresponding two-ring flip species β_2 which lies between 40, 40, 40 and $-40, 140, -40^\circ$, *i.e.* of 0, 90, 0°). Therefore it appears that in each case one ring flips first, followed by a second. In their study of helicity inversion in OPPh₃ Dunitz and co-workers¹² noted a similar deviation from the idealised geometry for the two-ring flip 'intermediate'.

The fragment which probably lies closest to the transition state for M-PPh₃ rotation has CSD refcode BUVSOA (see Fig. 3), the τ values (122.9, 242.9, 362.9°) of which place it almost exactly midway between the maxima of the τ distribution shown in Fig. 2. Perhaps surprisingly the ω values (133, 131, 133°) for BUVSOA are nearly perfectly propeller like and it falls close to the centre of the group II structures in, *e.g.*, Fig. 5. Other fragments which fall near the extremities of the τ distribution are all of group I if $\tau_B < 290^\circ$, and of group II if $\tau_B > 350^\circ$, the changeover occurring at or about $\tau_B = 315^\circ$ as noted above. There is no evidence as to the preferred mechanism of the helicity inversion which accompanies rotation about the M-P bond through values of $245 < \tau_B < 275^\circ$, but we may conjecture that the transition state for this process will have τ_B *ca.* 260° (and so τ_A *ca.* 140° and τ_C *ca.* 20°).

As was noted above, much of the interest in these complexes has focused on those species for which the contact atom of Z is an sp²-hybridised carbon atom. For the 34 cases for which this is the case and so Z is a ligand of the form C(Y)Q (where Y is often O or CR₂ and Q is often an alkyl group) the torsion angle $\nu = X-M-C-Y$ (in the range 0–360°) was calculated where Y was defined as the substituent most nearly *anti* to the XO ligand. Thus ν is variable (137–203°) but always fairly close to 180° (by definition it falls in the range 90–270°). Fig. 10 shows plots of ν *vs.* ω_B and τ_B with those cases in which Q is a double-bonded substituent circled for emphasis. There appears to be little effect of PPh₃ conformation (as indicated by either τ_B or ω_B) on the conformational preferences. The conformational preferences for ligands of this type have been the subject of extensive discussion and debate (see ref. 8 for a recent contribution). In molecular mechanics studies on complex **2** Davies *et al.*¹⁰ have recently noted that some flexibility in the acyl conformation is associated with conformational changes in the Fe-PPh₃ moiety.

To assess the generality of the model of phosphine π back bonding we described recently¹⁴ further analysis of the geometry of the M-PPh₃ fragment was carried out. The model predicts that increased M-P π bonding should cause shortening of the M-P bond, weakening and lengthening of the P-C bonds, and narrowing of the C-P-C angles in M-PPh₃ species as a consequence of increased occupancy of the pair of PPh₃ lowest unoccupied molecular orbitals (LUMOs) which contain some P-C σ^* character (see Fig. 11). If π donation is asymmetrical, *e.g.* the metal donates effectively only into one of the two PPh₃ LUMOs, then this model predicts that asymmetric distortions of the P-C lengths and C-P-C angles should occur. Such asymmetric donation would be expected for species **1** when Z is a poor π acceptor, in which case the only effective π -donor orbital on the M(η^5 -C₅R₅)(XO)Z fragment is the fragment highest occupied molecular orbital (HOMO) (mainly d_{yz} as illustrated in Fig. 11).^{4b} When the PPh₃ conformation has ring

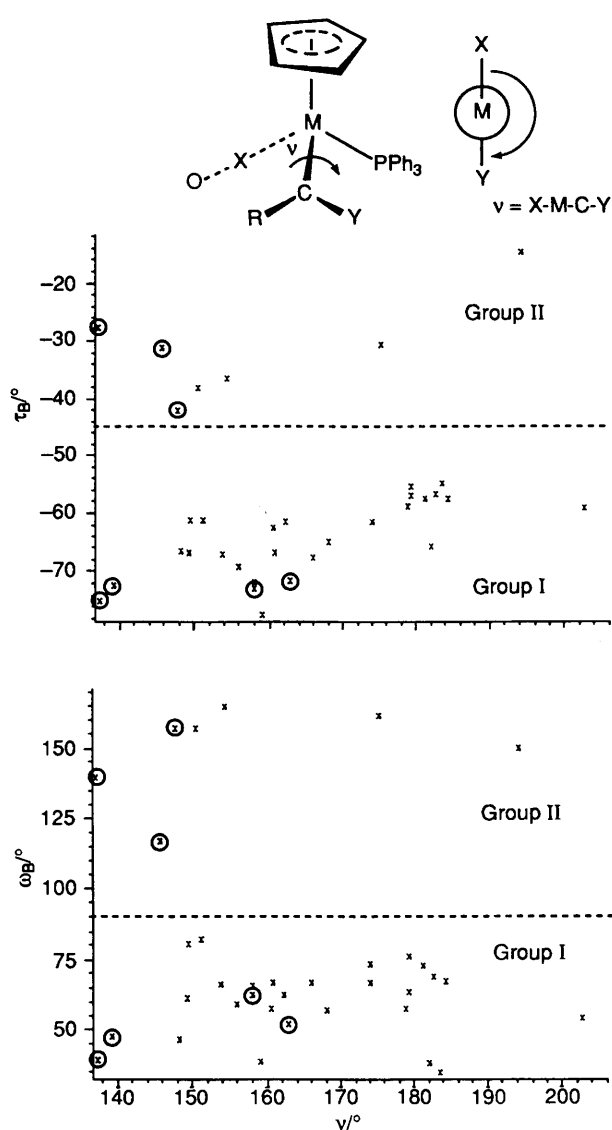


Fig. 10 Scattergram of torsion angle ν vs. τ_B and ω_B for structures in which the contact atom of ligand Z is an sp^2 -hybridised carbon

A *anti* to the XO ligand (as is predominantly the case) this orbital will π -donate exclusively into LUMO(2) causing weakening and lengthening of the P-C_{ipso} bonds for rings B and C (but not A) and narrowing of the C-P-C angle between rings B and C (but not of the other two C-P-C angles). These predictions may be tested against the numerical data available.

The 35 fragments for which M = Fe and the 22 cases for which M = Re were each divided into two classes on the basis of the π -acceptor ability of ligand Z (class A with Z a weak or non- π acceptor, e.g. alkyl, acyl, vinyl, phosphine or halide; class B with Z a strong π acceptor, e.g. carbene, vinylidene, carbonyl). Mean values of the Fe-P and Re-P bond lengths were calculated. These values (and the standard deviations of the distributions) are as follows: Fe-P Class A, 30 examples, 2.206(17); Class B, 5 examples, 2.241(1); Re-P Class A, 20 examples, 2.368(15), Class B, 2 examples, 2.420(10) Å. The presence of a systematic difference between the values for the M-P distances in these pairs of groups was then tested by a Mann-Whitney U-test.²² In each case (M = Fe and M = Re) the difference is significant at above the 99% level. Thus the presence of a strong π -acceptor ligand Z causes an increase in M-PPh₃ bond length, an observation consistent with a significant component of π bonding in the M-P bond in species 1.

For the 55 structures for which the conformation lies close to

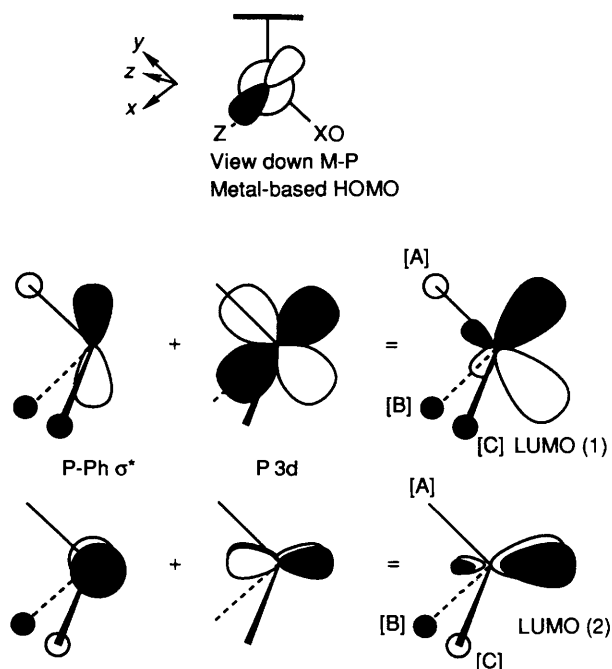


Fig. 11 Orbitals involved in M-P π bonding in species 1: the $M(\eta^5-C_5R_5)(XO)Z$ fragment HOMO and the PPh₃ ligand LUMOs. For the latter the P-C σ^* plus P 3d hybridisation is illustrated

that shown in Fig. 1 (*i.e.* with $\tau_A = 180 \pm 20^\circ$) a similar subdivision was made into classes C (Z = weak or non- π acceptor, 48 members) and D (Z = strong π acceptor, 7 members). Parameters Δ_{PC} and Δ_{CPC} were calculated for each fragment according to the relationships $\Delta_{PC} = P-C_A - 0.5(P-C_B + P-C_C)$ and $\Delta_{CPC} = C_C-P-C_B - 0.5(C_A-P-C_B + C_A-P-C_C)$ (where P-C_A is the P-C_{ipso} bond length for ring A, and C_A-P-C_B is the C_{ipso}-P-C_{ipso} bond angle formed between rings A and B). The values of Δ_{PC} and Δ_{CPC} were tested (Wilcoxon T-test)²² for systematic deviations from zero in the sense predicted above. These tests indicate that for group C (Z = weak π acceptor) Δ_{PC} tends to be negative (at better than 97.5% significance) and Δ_{CPC} negative ($>99.5\%$ significance) while for group D Δ_{PC} does not differ significantly from zero and Δ_{CPC} tends to be negative ($>99.0\%$ significance). Thus, as predicted, species for which highly asymmetric π donation would be expected show shorter P-C_A lengths and narrowed C_C-P-C_B angles. In contrast the cases with less (but usually non-zero) asymmetry of π donation show no significant asymmetry in P-C distances and less dramatic asymmetry in C-P-C angles.

Conclusion

The chief conclusions of this work relate to the preferred conformations of the PPh₃ ligand in species $S-[M(\eta^5-C_5R_5)(XO)Z(PPh_3)]$ 1 and the mechanisms by which they interconvert. There are two main diastereomer conformer types: group I which has *S* configuration at the metal and anticlockwise propeller (left-hand helix) conformation at PPh₃; and group II which has *S* configuration at the metal and clockwise propeller (right-hand helix) PPh₃. Group I structures predominate in the available dataset (56 to 18 in group II). In group I structures the Z ligand (at which much of the important chemistry of species 1 occurs) is shielded by phenyl ring B of the PPh₃ ligand which in the average conformation is rotated *ca.* 35° away from Z towards the XO ligand and which is face-on to Z. In group II structures phenyl B is edge-on to Z and face-on to XO, on average being rotated *ca.* 71° from Z. The PPh₃ ligand adopts conformations which support the assertion that rotation about the M-P bond is a relatively high-energy process which has a transition state having τ_B *ca.* 260° (and so τ_A *ca.* 140° and τ_C *ca.* 20°). Helicity inversion of PPh₃ can occur *without* full

rotation about the M–P bond and is accompanied by a rocking about the M–P bond in which τ_b passes through 315° and probably takes place by asynchronous two-ring flip mechanisms. One-ring flip mechanisms appear to be of higher energy than the two-ring alternatives but may be operative. Zero- and three-ring flip mechanisms appear to be of much higher energy. Full rotation about the M–P bond takes place with concomitant PPh₃ helicity inversion by an unspecified mechanism. The conformational model of Davies *et al.*¹⁰ (based on NMR spectroscopy and molecular mechanics*) successfully predicts many of these observations, which are based on experimental structural data. The PPh₃ groups show distortions in M–P and P–C distances and C–P–C angles consistent with significant and asymmetric M–P π bonding in those complexes for which Z is a poor π acceptor. This conclusion is in accord with a significant role for P–C σ^* orbitals in the π -acceptor capability of PPh₃.

Acknowledgements

We thank the many chemists and crystallographers who synthesised and determined the structures of the molecules studied, and Dr. G. Klebe for helpful discussions. We thank the SERC for a studentship (to S. E. G.). One of us (A. G. O.) thanks the Ciba-Geigy Fellowship Trust for the award of a Senior Research Fellowship and Professor D. Braga and his colleagues at the Dipartimento di Chimica 'G. Ciamician', Università di Bologna for their hospitality during a sabbatical stay in Bologna.

* Note added at proof: After submission of the present paper a further molecular mechanics study on [M(arene)LL'(PPh₃)] species was reported²³ whose conclusions are broadly consistent with the results presented here.

References

- Part 4, D. A. V. Morton and A. G. Orpen, *J. Chem. Soc., Dalton Trans.*, 1992, 641.
- Comprehensive Organometallic Chemistry*, eds. G. Wilkinson, F. G. A. Stone and E. W. Abel, Pergamon, Oxford, 1982; S. G. Davies, *Organotransition Metal Chemistry: Application to Organic Synthesis*, Pergamon, Oxford, 1982; J. P. Collman, L. S. Hegeudus, J. R. Norton and R. G. Finke, *Principles and Applications of Organotransition Metal Chemistry*, University Science Books, Mill Valley, CA, 1987.
- S. G. Davies, *Aldrichim. Acta*, 1990, **23**, 31 and refs. therein; S. G. Davies, I. M. Dordor-Hedgecock, R. J. C. Easton, S. C. Preston, K. H. Sutton and J. C. Walker, *Bull. Soc. Chim. Fr.*, 1987, 608 and refs. therein; S. G. Davies, *Pure Appl. Chem.*, 1988, **60**, 13 and refs. therein; S. G. Davies and J. I. Seeman, *Tetrahedron Lett.*, 1984, **25**, 1845.
- See, for example, (a) J. A. Gladysz, M. Marsi, A. T. Patton, D. R. Senn, C. E. Strouse and A. Wong, *J. Am. Chem. Soc.*, 1988, **110**, 6096; (b) S. Georgiou and J. A. Gladysz, *Tetrahedron*, 1986, **42**, 1109; (c) B. D. Zwick, M. A. Dewey, D. A. Knight, W. E. Buhro, A. M. Arif and J. A. Gladysz, *Organometallics*, 1992, **11**, 2673.
- See, for example, M. Brookhart, E. W. Goldman, Y. Liu, D. A. Timmers and G. D. Williams, *J. Am. Chem. Soc.*, 1991, **113**, 927; M. Brookhart, G. R. Husk and J. R. Tucker, *J. Am. Chem. Soc.*, 1983, **105**, 258; L. L. Campbell, T. C. Flood, J. E. Jensen and S. Nakanishi, *J. Organomet. Chem.*, 1983, **244**, 61; H. Brunner, B. Hammer, I. Bernal and M. Draux, *Organometallics*, 1983, **2**, 1595; R. W. Fengl, L. S. Liebeskind and M. E. Welker, *J. Am. Chem. Soc.*, 1986, **108**, 6328; L. S. Liebeskind and M. E. Welker, *Tetrahedron Lett.*, 1984, **25**, 4341.
- (a) S. G. Davies and J. I. Seeman, *J. Am. Chem. Soc.*, 1985, **107**, 6522; (b) S. G. Davies, B. K. Blackburn, K. H. Sutton and M. Whittaker, *Chem. Soc. Rev.*, 1988, **17**, 147 and refs. therein.
- G. S. Bodner, S. Georgiou, J. A. Gladysz, A. T. Patton, D. E. Smith, C. E. Strouse, W. Tam and W. Wong, *Organometallics*, 1987, **6**, 1954; A. G. Constable, O. Eisenstein, J. A. Gladysz, W. A. Kiel, G.-Y. Lin, F. B. McCormick and C. E. Strouse, *J. Am. Chem. Soc.*, 1982, **104**, 4865; G. S. Bodner, S. J. Geib, S. Georgiou, J. A. Gladysz, W. G. Hatton, P. C. Heah, J. P. Hutchinson, A. L. Rheingold and D. E. Smith, *J. Am. Chem. Soc.*, 1987, **109**, 7688; W. E. Buhro, S. Georgiou, J. A. Gladysz, J. P. Hutchinson and B. D. Zwick, *J. Am. Chem. Soc.*, 1988, **110**, 2427.
- S. Shambayati, W. E. Crowe and S. L. Schreiber, *Angew. Chem., Int. Ed. Engl.*, 1990, **29**, 256; see also, S. G. Davies and A. J. Smallridge, *J. Organomet. Chem.*, 1990, **397**, C13.
- S. G. Davies, B. K. Blackburn and M. Whittaker, *Chemical Bonds—Better Ways to Make and Break Them. Stereochemistry of Organometallic and Inorganic Compounds*, ed. I. Bernal, Elsevier, Amsterdam, 1989, vol. 3, p. 141 and refs. therein.
- S. G. Davies, A. E. Derome and J. P. McNally, *J. Am. Chem. Soc.*, 1991, **113**, 2854.
- P. Murray-Rust and S. Motherwell, *Acta Crystallogr., Sect. B*, 1978, **34**, 2534.
- E. Bye, W. B. Schweizer and J. D. Dunitz, *J. Am. Chem. Soc.*, 1982, **104**, 5893.
- F. H. Allen, M. J. Doyle and R. Taylor, *Acta Crystallogr., Sect. B*, 1991, **47**, 29, 41, 50; F. H. Allen, M. J. Doyle and T. P. E. Auf der Heyde, *Acta Crystallogr., Sect. B*, 1991, **47**, 412.
- N. G. Connelly and A. G. Orpen, *J. Chem. Soc., Chem. Commun.*, 1985, 1310; *Organometallics*, 1990, **9**, 1206; B. J. Dunne, R. B. Morris and A. G. Orpen, *J. Chem. Soc., Dalton Trans.*, 1991, 653.
- S. E. Garner and A. G. Orpen, *Acta Crystallogr., Sect. A*, 1990, **46**, C360.
- H. Brunner, B. Hammer, C. Krüger, K. Angermund and I. Bernal, *Organometallics*, 1985, **4**, 1063.
- F. H. Allen, O. Kennard and R. Taylor, *Acc. Chem. Res.*, 1983, **16**, 146; F. H. Allen and J. E. Davies, in *Crystallographic Computing 4*, eds. N. W. Isaacs and M. R. Taylor, Oxford University Press, Oxford, 1988.
- P. Murray-Rust and J. Raftery, *J. Mol. Graphics*, 1985, **3**, 50, 60.
- J. D. Dunitz and H.-B. Bürgi, *Acta Crystallogr., Sect. B*, 1988, **44**, 445.
- International Tables for Crystallography*, Reidel, Dordrecht, 1983, vol. A.
- A. K. Colter, R. J. Kurland and I. I. Schuster, *J. Am. Chem. Soc.*, 1965, **87**, 2279.
- S. Siegel, *Non-Parametric Statistics*, McGraw-Hill, New York, 1956.
- J. Polowin, S. C. Mackie and M. C. Baird, *Organometallics*, 1992, **11**, 3724.

Received 4th September 1992; Paper 2/04771C